# Synthesis of Monodisperse High-Aspect-Ratio Colloidal Silicon and Silica Rods

**ARTICLE** *in* LANGMUIR · JANUARY 2005

Impact Factor: 4.46 · DOI: 10.1021/la048817j · Source: PubMed

# Synthesis of Monodisperse High-Aspect-Ratio Colloidal Silicon and Silica Rods

Carlos M. van Kats,[†,‡] Patrick M. Johnson,*[,†,‡,§]
Jan E. A. M. van den Meerakker,[||] and Alfons van Blaaderen*[,‡]

*Soft Condensed Matter, Debye Institute, Ornstein Laboratory, Princetonplein 5, 3584 CC Utrecht, The Netherlands, and Philips Research, Prof. Holstlaan 4, 5656 AA Eindhoven, The Netherlands*

*Received May 13, 2004. In Final Form: August 13, 2004*

We describe the synthesis and the physical properties of suspensions of colloidal silicon and silica rodlike particles. In addition to pure silicon and pure silica rods, we have also synthesized silicon rods with a silica shell and silica rods with a fluorescent silica layer. Pre-patterned p-type (100) silicon wafers were electrochemically etched in electrolyte solutions containing hydrogen fluoride. By the current density being varied while etching, macropores were etched with controllable modulated pore diameters. These silicon structures were transformed into rods with indentations 5.5 $\mu$m apart and with lengths up to 100 $\mu$m using iterative oxidation in air and dissolution of the silica by HF. Complete oxidation of these rods was also achieved. Sonication of the modulated rods resulted in monodisperse particles of 5.5 $\mu$m length and 300 nm width. A high yield of $10^{12}$ particles, or more, is possible with this method. At high concentrations, these particles show nematic ordering in charge-stabilized suspensions. The oxidized silica outer layer of the silicon rods makes the further growth of silica in solution or on a wafer possible. This allows for control of the particles' interaction potential. Labeling with a fluorescent dye and index matching of the complete silica rods enable the study of concentrated dispersions quantitatively, on a single particle level, with confocal microscopy. Because of their high refractive index in the near-IR, the nematic phases of rods with a silica core are also interesting for photonic applications.

## I. Introduction

Colloidal rods are interesting as condensed matter model systems and for applications[1] because of anisotropy in the particle properties and their ability, at high aspect ratios, to form liquid crystalline phases.[2]

Recent fundamental studies have shown that a combination of index matching and fluorescent labeling make it possible to quantitatively study both the structure and dynamics of concentrated colloidal dispersions of spheres with confocal microscopy on a single particle level.[3−7] The extensive knowledge that is available on the modification of the surface of silica makes it possible to tune interactions from long-range repulsive[8] to hard-sphere-like[3,4] to even dipolar.[9] Since such fundamental real-space studies have only been carried out using colloidal spheres, it is our motivation to extend these studies to rodlike colloidal model systems with tunable aspect ratios.

On the applied side, semiconductor colloidal rods in particular are increasingly important as functional components for new types of electrooptical, electromechanical, and sensing devices in microelectronics.[10] We explore the photonic properties of (liquid) crystalline phases of rodlike particles with a silicon core. Silicon does not absorb in the near-IR and has a very high refractive index ($n = 3.5$ at $\lambda = 1.5$ $\mu$m).[11] Photonic (liquid) crystals made from anisotropic particles have until now scarcely been explored.[12−14]

The theory of the liquid crystalline behavior of rodlike colloidal particles has consistently preceded the experimental study of these systems. As early as 1949, Onsager showed that a system of long, hard rods interacting with purely repulsive forces exhibits orientational (nematic) order at critical densities far from the closest packing.[15] The Onsager theory was extended to polydisperse solutions and soft interactions by several groups.[2,16] Computer simulations have further shown that not only nematic phases but also smectic and crystalline phases can occur.[17−19] Experimental studies on rodlike colloidal model systems are far less numerous than that on spheres. Nevertheless, examples of isotropic−nematic phase behavior have been observed with several different (more-

* Authors to whom correspondence should be addressed. E-mail: patrick.johnson@simmons.edu (P.M.J.), a.vanblaaderen@phys.uu.nl (A.v.B.).
† Both authors (C.M.v.K. and P.M.J.) contributed equally.
‡ Ornstein Laboratory.
§ Present address: Physics Department, Simmons College, 300 the Fenway, Boston, MA 02115-5898.
|| Philips Research.

(1) Xia, Y.; Yang, P.; Sun, Y.; Wu, Y.; Mayers, B.; Gates, B.; Yin, Y.; Kim, F.; Yan, H. *Adv. Mater.* **2003**, *15*, 353.
(2) Vroege, G. T.; Lekkerkerker, H. N. W. *Rep. Prog. Phys.* **1992**, *55*, 1241.
(3) van Blaaderen, A.; Wiltzius, P. *Science* **1995**, *270*, 1177.
(4) van Blaaderen, A.; Ruel, R.; Wiltzius, P. *Nature* **1997**, *385*, 321.
(5) Kegel, W. K.; van Blaaderen, A. *Science* **2000**, *287,* 290.
(6) Gasser, U.; Weeks, E. R.; Schofield, A.; Pusey, P. N.; Weitz, D. A. *Science* **2001**, *292*, 258.
(7) Yethiraj, A.; van Blaaderen, A. *Nature* **2003**, *421*, 513.
(8) van Blaaderen, A. *MRS Bull.* **1998**, ***23***, 39.
(9) Dassanayake, U.; Fraden, S.; van Blaaderen, A. *J. Chem. Phys.* **2000**, *112*, 3851.
(10) Cui, Y.;. Lieber, C. M. *Science* **2001**, *291*, 851.
(11) Dargys A.; Kudrotas, J., *Handbook on Physical Properties of Ge, Si, GaAs and InP*; Academic Press: New York, 1975.
(12) Yin, Y.; Xia, Y. *Adv. Mater.* **2001**, *13*, 267.
(13) Velikov, K. P.; van Dillen, T.;. Polman, A.; van Blaaderen, A. *Appl. Phys. Lett.* **2002**, *81*, 838.
(14) Birner, A.; Wehrspoon, R. B.; Goesele U. M.; Busch, K. *Adv. Mater.* **2001**, *13,* 377.
(15) Onsager, L. *Ann. N. Y. Acad. Sci.* **1949**, *51*, 627.
(16) Stroobants, A.; Lekkerkerker, H. N. W.; Odijk, T. *Macromolecules* **1986**, *19*, 2232.
(17) Frenkel, D.; Mulder, B. M. *Mol Phys.* **1985**, *55*, 1171.
(18) Frenkel, D.; Lekkerkerker, H. N. W.; Stroobants, A. *Nature* (London) **1988**, *332*, 822.
(19) Bolhuis, P. G.; Stroobants, A.; Frenkel, D.; Lekkerkerker, H. N. W. *J. Chem. Phys.* **1997**, *107*, 1551.

10.1021/la048817j CCC: $27.50 
Published on Web 10/22/2004

or less-stiff) organic rods (FD-, TMV-viruses, polyglutamates, DNA)[16,20,21] and inorganic materials (vanadium pentoxide ($V_2O_5$), $\beta$−ferric oxyhydroxide ($\beta$−FeOOH), boehmite (ALOOH)).[22−25] The first real-space observation of self-ordering of liquid crystals from rodlike colloidal particles on a single particle level has recently been reported by Maeda.[26] However, these observations are not yet quantitative. The high refractive index of $\beta$-ferric oxyhydroxide will make it hard to carry out real-space analysis on this system.

In this article, we describe the synthesis of stable dispersions of silicon rods, their conversion to pure silica, and their labeling with a fluorescent dye. Our synthetic method yields large enough quantities of particles to allow the study of the dynamic behavior of concentrated dispersions of rods.

Silicon rods of sizes from a few nanometers to micrometers have recently been produced by several different methods. Various groups have reported making silicon nanowires via laser ablation,[27] where single crystalline rods grow from an oversaturated nanocolloid of catalyst material (e.g., gold). Chemical vapor deposition (CVD) of $SiH_2Cl_2$ [28] on $TiSi_2$ islands has also been performed, allowing smaller silicon wires to be grown with nanometer precision. Silicon rods have also been made via a template-directed synthesis,[29] where particles nucleate and grow in supporting channels in anodic alumina membranes. For a survey of other methods, see the papers of Xia and co-workers.[1,30]

While these methods may be useful in a number of applications, they are not suitable for producing colloidal model systems because the polydispersity of the rod lengths is very high and/or the yield is too low. In our synthesis method, we begin by creating pores by etching into silicon. When widened, the pores start to overlap, resulting in long rods. In addition, we modulate the width of the pores creating rods with regularly spaced indentations. The advantage of our method is that we have a high level of control over the particle dimensions. Moreover, we can obtain a relatively high yield of particles ($10^{12}$) because the method is essentially 3D. We can estimate the maximum possible rod yield as follows: the wafers contain ∼4 billion pits. The maximum possible depth of etched pores is ∼0.5 mm. The minimum rod length is several micrometers. This suggests a maximum yield of $\sim 10^{12}$ particles.

Lehmann and co-workers demonstrated for relatively small n-type wafers that modulating the light intensity during electrochemical etching resulted in modulated macropore formation.[31] In our experiments, we show that modulations of pore formation can also be achieved with p-type silicon by modulating the applied current. We have achieved structures with uniform lengths and diameters, up to 100 $\mu$m deep. This ability to etch modulated rods deep into the wafer allows us to use an entire 6-in. wafer to obtain a relatively high yield of particles. As far as we know, this is the first example of modulated pore etching in p-type silicon.[32]

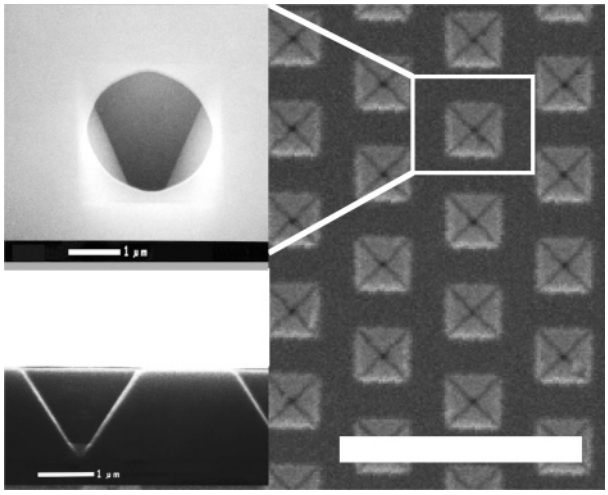

**Figure 1.** The pit pattern of a silicon wafer before electrochemical etching (top view, right; diagonal side-view, top left; and side-view of a cleaved wafer, bottom left). Etch pits are 3.5 $\mu$m apart. Each pit has an inverse pyramidal shape (due to anisotropic etching with KOH) with a width of 1.5 $\mu$m and a depth of 1 $\mu$m. A 6-in. silicon wafer contains ∼4 billion pits. The scale bar on the right represents 10 $\mu$m, while the scale bars on the left represent 1 $\mu$m.

**The Electrochemical Etching of Silicon in HF Solutions.** Macroporous etching of silicon, first reported by Lehmann and co-workers,[33,34] has been used to make photonic crystals,[14] micropumps and membranes,[35] and solid-state capacitors from 6-in. wafers.[36] In this article, we use similar techniques to make silicon nanowires from silicon wafers.

Under anodic polarization in HF solution, silicon is oxidized and dissolves. Positive charge carriers (holes) are required to drive the electrochemical reaction. In p-type silicon, holes are available in the valence band at room temperature. In n-type silicon, electron−hole pairs can be created by illuminating the semiconductor.[37]

Electrochemical etching at strongly positive potentials can be used to create macropores. To control the pore spacing and pore dimensions, pre-patterned silicon wafers can be used. Regularly spaced anisotropically etched macropores can be formed with patterned structures containing pre-etched indentations[38] (Figure 1).

Once electrochemical etching begins, the holes are driven toward the front of the patterned wafer by the applied potential. The pores will begin etching at the tip of the inverted pyramid in the direction parallel to the applied electric field. In this way, unidirectional etching is realized and a highly regular array of macropores can be formed. In p-type silicon, the diameter of the formed macropores can be controlled by the applied current.

(20) Fraden, S.; Maret, G.; Caspar, D. L. D.; Meyer, R. B. *Phys. Rev. Lett.* **1989**, *63*, 2068.
(21) Tracey, M. A.; Pecora, R. *Macromolecules* **1992**, *25*, 337.
(22) Pelletier, O.; Davidson, P.; Bourgeaux, C. Livage, C. *J. Europhys. Lett.* **1999**, *48*, 53.
(23) Maeda, H.; Maeda, Y. *Langmuir* **1995**, *11*, 1446.
(24) Buining, P. A.; Philipse, A. P.; Lekkerkerker, H. N. W. *Langmuir* **1994**, *10*, 2106.
(25) van Bruggen, M. P. B.; Dhont, J. K. G.; Lekkerkerker, H. N. W. *Macromolecules* **1999**, *32*, 2256.
(26) Maeda, H.; Maeda, Y. *Phys. Rev. Lett*. **2003,** *90*, 18303.
(27) Morales, A. M.; Lieber, C. M. *Science* **1998**, *279*, 208.
(28) Kamins, T. I.;. Williams, R.S; Chen, Y.; Chang, Y; Chang, Y. A. *Appl. Phys. Lett.* **2000**, *76*, 562.
(29) Lew, K. K.; Reuther, C.; Carim, A. H.; Redwing, J. M.; Martin, B. R. *J. Vac. Sci. Technol. B* **2002**, *20*, 389.
(30) Yin, Y.; Gates, B.; Xia, Y. *Adv. Mater.* **2000**, *12*, 1426.
(31) Lehmann, V. *J. Electrochem. Soc.* **1993,** *140*, 2836.
(32) van den Meerakker J. E. A. M., van Kats C. M., van Blaaderen, A. et al., PHNL021185WO (patent application no. 02079837.7).
(33) Lehmann, V. *Electrochemistry of Silicon*; Wiley VCH: Weinheim, 2002.
(34) Lehmann V.; Ronnebeck, S. *J. Electrochem. Soc.* **1999**, *148,* 2968.
(35) Müller, F.; Birner, A.; Schilling, J.; Gösele, U.; Kettner, C.; Hänggi, P. *Phys. Status Solidi A* **2000**, *182*, 585.
(36) van den Meerakker, J. E. A. M.; Elfrink, R. J. G.; Roozeboom F.; Verhoeven, J. F. C. M. *J. Electrochem. Soc.* **2000**, *147*, 2757.
(37) Zhang, X. G. *Electrochemistry of Silicon and its oxide*; Kluwer Academic/Plenum Publishers: New York, 2001.
(38) van den Meerakker, J. E. A. M.; Elfrink, R. J. G.; Weeda W. M.; Roozeboom, F. *Phys. Status Solidi A* **2003**, *197*, 57.

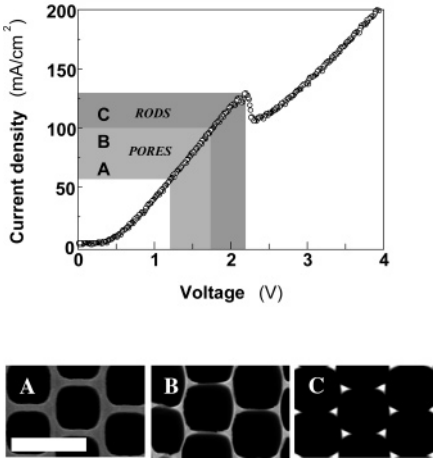


**Figure 2.** Typical current-to-voltage plot. The ranges of expected rod formation (upper part (dark gray) at higher current densities) and pore formation (lower part, light gray) are marked. Figure 2 A–C: top view of different stages of pore etching (scale bar represents 2 $\mu$m). Etched structures with (A) macropores and thick walls, (B) broad macropores and thin walls, and (C) overlapping macropores which form rods. The SEM pictures correspond to the ranges A, B, and C in the upper graph. At higher current densities, electropolishing of the wafer occurs.

Increasing the total applied current increases the pore size. At a high applied current, the pores start to overlap and silicon rods are formed. Under the right conditions, highly anisotropic pores of up to micrometers in diameter can be etched in p-type silicon up to 400 $\mu$m in depth.[39] If a high enough current is applied, the pores completely overlap and the whole surface of the wafer becomes etched. This results in electropolishing of the silicon surface. These different stages in etching are illustrated in Figure 2. Modulating the current density can modulate the diameter of these pores during the etching process. This was shown previously for n-type silicon wafers by modulating the light intensity.[31,35] The process of etching uniform macropores is well explained for n-type silicon, for which the concentration of charge carriers, and thus the diameter of the pores, can be regulated by light-induced electron–hole pair formation at constant applied potential.[31,40] For p-type silicon, the physical and chemical processes that regulate the etching process are not yet well understood.

## II. Materials and Methods

**Materials.** All chemicals and solvents were used as received without further purification. Ethanol (technical grade, containing 5% methanol), hydrogen fluoride (HF, 50%, Merck), a 25% w/w cetyltrimethylammonium chloride (CTAC) solution in water, potassium sulfate ($K_2S0_4$, Aldrich), and demineralized water were used in the etching setup. Tetraethoxysilane (TEOS), 3-(aminopropyl)triethoxysilane (APS), fluorescein isothiocyanate (FITC ,Fluka), ammonia 25% w/w, and ethanol p.a. (Merck) were used for the silica growth on the rods. Dimethyl sulfoxide (DMSO, Fluka) was used to index match the silica rods under the confocal microscope. Biorad AG501-X8 mixed ion-exchange resin was used to deionize the water.

**Instrumentation.** The current was controlled via a LabView computer program, with a Philips power source (PM2811). Scanning electron microscopy (SEM) images were taken on a Philips XL30FEG microscope. High-resolution transmission electron microscopy (HRTEM) was performed on a TECNAI20. Silicon wafers were oxidized in air by heating in a Carbolite ESF oven. Confocal microscopy images were taken on a Leica DM IRB confocal microscope. Samples were supercritically dried on a Bal-tec critical point dryer (CPD030). Samples were centrifuged with a Hettich Rotina 46S table centrifuge and sonicated with a Bransonic 8510 sonicator, operating at a power of 250 W with a frequency of 44 kHz.

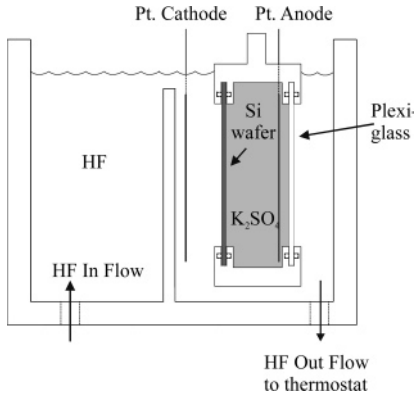


**Figure 3.** The experimental setup: a container with 8 L of HF solution in an ethanol water mixture that is pumped via a thermostat to control the temperature. The closed plexiglass container with potassium sulfate electrolytic solution keeps the electric field uniform over the whole silicon wafer.

**The Etching Setup.** In our experiment, we used 6-in. p-type (boron doped) (100) silicon wafers with a resistivity of 10–20 Ω cm with pre-etched indentations on one side (see Figure 1). A pattern with a hexagonal array of ~4 billion holes in the etch mask was obtained as described in earlier publications[36] by standard lithographic techniques. This patterning was realized by exposing a wafer to an 8.8 M KOH solution at 70 °C for 8 min using a $Si_3N_4$ mask. These pre-etched pyramidal holes had widths of 1.5 $\mu$m and a pitch of 3.5 $\mu$m (see Figure 1). Before the pore etching started, the mask was removed in concentrated $H_3PO_4$ at 140 °C.

For large (6 in.) silicon wafers, a number of steps were taken to ensure a uniform electric field, temperature, and HF flow rate over the entire wafer surface. An electrolyte solution of HF, CTAC, ethanol, and water was thermostated at a temperature of 30 °C (unless otherwise stated) in a polycarbonate container by pumping the solution via a Teflon-coated pump through a temperature-controlled water bath (see Figure 3).

The 6-in. silicon wafer was held in a polypropylene container filled with a 0.16 M $K_2SO_4$ electrolyte solution, which acted as an electrolytic back contact of the wafer. In this way, a uniform electric field over the silicon wafer was obtained. The chamber contained a 137 cm$^2$ Pt grid as the anode. The cathode counter electrode was a Pt sheet of 196 cm$^2$ positioned parallel to the Si wafer at a distance of about 3 cm.[36] The electrolytic HF solution was pumped via a thermostated bath over the cathode sheet along the silicon wafer. This pumping regulates the temperature of the solution, homogenizes the HF concentration, and facilitates the flow of hydrogen gas created at the wafer surface during etching. Macropores were etched by generating an electric potential across the electrodes.

The optimum etching conditions were determined from a current-to-voltage diagram (IV-curve (see Figure 2)). The current was measured while the potential across the wafer was decreased at a scan rate of 10 mV/s. The resulting IV-curve peaks at the point when electropolishing begins. Pores or rods were obtained by choosing an appropriate applied current relative to this peak.

We performed etching experiments with an electrolyte solution of 7.9 L containing 1300 mL of HF (4.7 M), 2600 mL of ethanol (5.7 M), 100 mL of the 25% CTAC solution, and 3900 mL of demineralized water. The polypropylene container holding the platinum anode and the silicon wafer was filled with a 0.16 M $K_2SO_4$ electrolyte solution. Typical current densities used for a 6-in. wafer (with ~133 cm$^2$ available surface area for etching) were 100 mA/cm$^2$ for making rods and 67 mA/cm$^2$ for making macropores. We etched 6-in. silicon wafers to give varying rod thicknesses by alternating the current density between 13.5 and 9 A, 5–20 times for 1 min each period.

(39) Chao, K. J.; Kao, S. C.; Yang, C. M.; Hseu, M. S.; Tsai, T. G. *Electrochem. Solid-State Lett.* **2000**, *3*, 489.

(40) van den Meerakker, J. E. A. M.; Mellier, M. R. L. *J. Electrochem. Soc.* **2001**, *148,* G166.

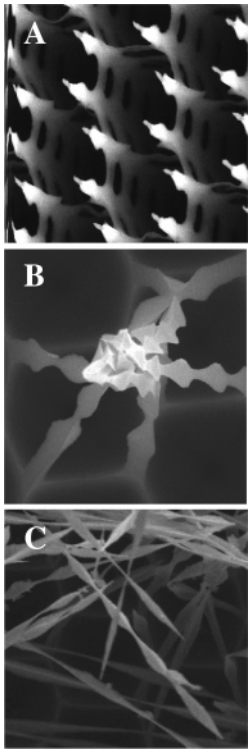


**Figure 4.** Examples of etched silicon wafers: (A) the result after etching in the setup, (B) the result after two oxidation/etch cycles, and (C) the result after four oxidation/etch cycles. The SEM pictures are taken at different viewing angles. Thin particles tend to bend on the wafer; therefore, particles can be seen in different directions. After four oxidation cycles, the particles are thin enough to be rinsed off without sonication.

A few tests were performed at 25 °C with the same solutions to explore the influence of temperature on the etch conditions.

**From Macroporous Silicon Wafers to Silicon/Silica Rods in Suspension.** The structure obtained after modulation of current density on large 6-in. wafers can be repeatedly oxidized thermally and etched in HF to create modulated rods with desired dimensions. This is illustrated in Figure 4. The sample etched with alternated current densities during etching was put in a Carbolite ESF oven at 950 °C for 15 min. The silica layer formed was subsequently removed by etching for 15 min in 3.75 M HF.

After fine-tuning the average thickness, the rods were washed off the wafer by rinsing with water or (more vigorously) by ultrasonication in distilled water.

We grew silica on the rods using well-known methods. The silicon rods that were rinsed off and sonicated were transferred to ethanol and a thin silica layer was grown on the particles. In a typical fluorescent silica growth experiment,[41] the sonicated rods ($\sim 2 \times 10^9$) were dispersed in 0.5 mL of ethanol containing 50 $\mu$L of 25% ammonia. A fresh mixture of 44 $\mu$L of TEOS and the FITC-APS dye (30.6 $\mu$g of FITC reacted with 0.18 $\mu$L of APS in 250 $\mu$L of ethanol overnight) were added at once and stirred for 16 h. A fluorescent layer of ~50 nm was grown on the rods. Secondary-nucleated particles were removed by repeated centrifugation (15 min, 750 rpm).

To create all-silica particles, we thermally oxidized silicon rods completely on the wafer. However, if the wafer was dried in air, drying forces would lead to bending and bunching of the rods and, ultimately, sintering during thermal oxidation. For this reason, we dried the wafer supercritically. Due to the small size of our supercritical dryer, a 1 cm$^2$ piece of wafer was used. This supercritically dried wafer was then thermally oxidized for 16 h at 950 °C.

After this oxidation step, a fluorescent layer of silica was grown on the rods on this piece of a wafer with a method described by Vossen et al.[42] The piece of wafer was put in a 1.1 vol% solution of silica spheres with a diameter of 1030 nm, containing 1.0 mL of 25% ammonia in 15.0 mL of ethanol. To grow a layer of 50 nm fluorescent silica on the rods, 395 $\mu$L of TEOS was added to this dispersion, together with the FITC-APS dye (1.3 mg of FITC coupled to 8.4 $\mu$L of APS in 250 $\mu$L of ethanol stirred overnight).

Stable suspensions of rods in water were sedimented (in normal gravity) at different concentrations. To achieve low ion concentrations, water was deionized with an ion-exchange resin.

## III. Results and Discussion

**Electrochemical Etching of p-Type Silicon Wafers.** The different regimes we obtained during the electrochemical etching are shown in Figure 2: macropores are formed (case A), macropores are broadened (case B), and macropores start to overlap in such a way that rods are formed (case C). When currents higher than 150 mA/cm$^2$ were applied, the wafer was electropolished. By the proper choice of current density, we could form either pores or rods.

Alternating the current density during etching modulated the pore width; therefore, in our samples, we find regions where pores overlap (rods) and regions where pores do not overlap. We etched with a square-wave current alternating between 100 and 67 mA/cm$^2$ for 1 min each. While the pore diameter is modulated with the same frequency as the current, sharp steps in the diameter were not observed. Instead, a gradual transition from wide to thin pores (and vice versa) was observed. We analyzed SEM images of the electrochemically etched wafers to measure the polydispersity in modulation lengths and pore diameters. Under ideal etch conditions, each modulation length was extremely reproducible and independent of depth or location on the wafer. This can be seen from the constant slope of etching depth versus the number of complete modulation cycles in Figure 5. We also found the local variations in pore diameter to be immeasurably small, i.e., pores within a few mm of each other were the same size to within tens of nm. Also, these pores did not narrow or widen with depth. Over larger distances across the wafer, slight variations in diameter on the order of 100 nm could be seen. Regions of uniform pore diameter formed alternating rings with widths of ~0.5 cm. This ring pattern suggests that the diameter polydispersity was caused by variations in the silicon induced during the wafer growth, e.g., variations in boron doping concentration. A locally higher or lower dopant level can cause local differences in etching kinetics. For instance, a locally higher dopant level could cause a higher flux of holes to the pore tips, which gives wider pores or smaller rods since, locally, more silicon will be etched.

Lehmann showed that, for electrochemical etching of pores in at n-type wafers, the etch rate slowly decreased in depth.[31] This was attributed to a decrease in the HF concentration at the pore tips because of diffusion. In our experiments, in which we used etch rates up to 6.5 times higher, no decrease was observed, as can be seen from the straight line in etch depth as a function of the number of modulation cycles in Figure 5. Even at an etch depth of 100 $\mu$m, the HF diffuses fast enough to the pore tips. However, we also performed similar experiments at lower temperature (25 °C), and surprisingly, we always found widening of pores, even at etch depths of 10−20 $\mu$m. Under these conditions, it was not possible to modulate the pores in a regular fashion; therefore, we could not determine whether the etch rate changed with the widening of the pores.

(41) van Blaaderen, A.; Vrij, A. *Langmuir* **1992**, *8*, 2921.

(42) Vossen, D. L. J.; de Dood, M. J. A.; van Dillen, T.; Zijlstra, T.; van der Drift, E.; Polman, A.; van Blaaderen, A. *Adv. Mater.* **2000**, *12*, 1434.

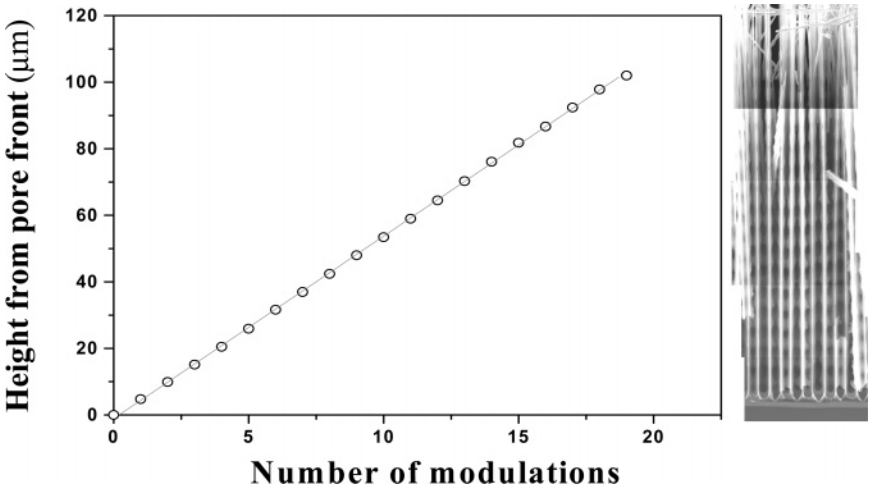


**Figure 5.** Silicon etched to a depth of ~100 $\mu$m. Twenty modulations are visible. A plot of the height of the rods at the pore front versus the number of modulations shows a constant etching rate, with a modulation length of 5.5 $\mu$m. The top of the etched structure is damaged due to cleaving the sample for SEM observation.

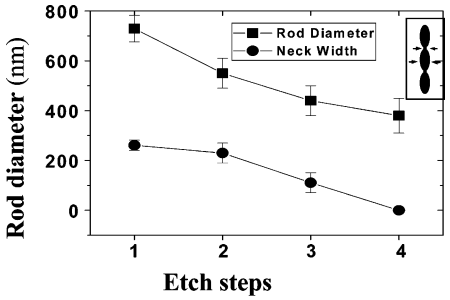


**Figure 6.** Thickness of the rods as a function of the number of etch steps. One etch step consists of oxidation at 950 °C and etching with 3.75 M HF. The error bars are given by the polydispersity in thickness, caused mainly by the nonconstant doping level. The arrows in the inset indicate the locations at which the rod diameter and neck width were measured.

**Fine-Tuning Silicon Structures.** To increase the pore size further and produce isolated modulated rods, we oxidized the structures in air and dissolved the silica in 3.75 M HF. In the example shown in Figure 4, the oxidation/HF-dissolution cycle was repeated 4 times until the desired rod thickness was obtained. In each cycle, the average diameter of the silicon rods was reduced by ~125 nm. Figure 6 shows a plot of the rod diameter after each oxidation/HF-etch cycle. This method allows us to control the diameter to within tens of nanometers. Figure 4 shows that thin rods (maximum rod diameters of 400 ± 50 nm) were etched from initially thick silicon structures (maximum rod diameters of 725 ± 50 nm). While Figure 4 shows results for rods produced with 5 modulation cycles, identical results were obtained with rods after 20 modulation cycles (Figure 5).

After the desired rod thickness was achieved, the particles could be removed by agitating the wafer in water or ethanol. The intensity of the agitation determined the amount of rods that were removed from the wafer. For example, ultrasonication of the wafer in water caused all of the rods to break off from the wafer within seconds. By contrast, applying a mild water jet to the surface of the wafer caused only the thinnest rods to fall off. This result proved to be useful for reducing the polydispersity in rod diameter. Using a mild water jet to rinse off the rods allowed rings of the thinnest rods to be removed from the wafer, while rings of thicker rods remained attached. Following a rinse, the thicker rods that remained on the wafer could be further etched. In this way, all of the rods

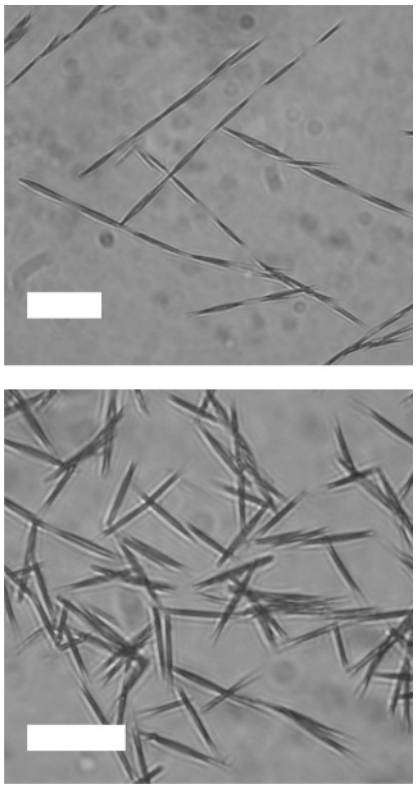

**Figure 7.** Breaking up rods at the indentations: the rods are removed from the silicon wafer by flushing with water. The scale bar represents 5 $\mu$m. Upper picture: optical microscope picture taken after only flushing the silicon wafer with water, no sonication. Lower picture: optical microscope picture taken after 60 min of sonicating, which results in single particles.

removed from the wafer had a minimum diameter of 100 ± 25 nm and an average diameter of 250 ± 50 nm. This rinsing method reduced but did not eliminate the diameter polydispersity. In the future, a more homogeneous boron doping process could further improve the pore diameter monodispersity.

Once removed from the wafer, the modulated rods were transformed into individual rods by sonication. Sonication causes the rods to break at the thinnest points. After a short period (less than 10 min) of sonication in an ultrasonic bath, the suspension still contains many rods that have more than one modulation (Figure 7). A longer

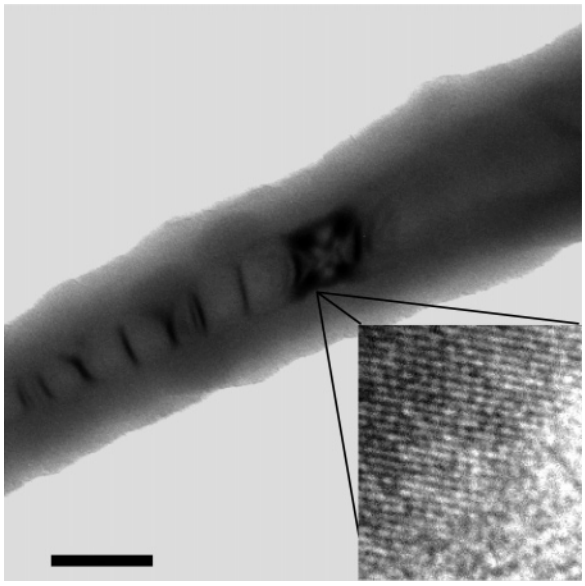

**Figure 8.** HRTEM of a silicon rod on which silica was grown (scale bar represents 200 nm). The inset is a further magnification of the boundary between the crystalline silicon and the amorphous silica layer. The crystalline part shows different dark regions in the HRTEM picture, probably caused by stress exerted by thermal silica during thermal oxidation. Stress in the crystal plane and an unknown viewing angle hinders the exact determination of the lattice spacing.

sonication period (60 min) resulted in a more monodisperse rod dispersion where more than 95% of the particles have only one modulation length (Figure 7). The dimensions of this final rod dispersion are 5.5 $\mu$m length and 250 nm width, with a size polydispersity of ~25%. Polydispersity in length is mainly caused by those particles that do not break exactly at the thinnest points.

The variation in length of the final rods might be improved by shortening the high-current-density period during etching. With shorter periods of high current, the thinnest regions of the modulated rod will become shorter. In this way, the thin necks where segmented rods will break during sonication could be determined more precisely, resulting in a higher monodispersity. Since we already saw that the etching of rods does not immediately follow the block current that is imposed, there are limitations to the minimal length of the periods of the alternations of the current. Too drastic of a change in current density may also result in a sudden death of formed macropores during etching. This effect has been observed in the etching of n-type silicon.[31] We have not seen this effect at p-type silicon under comparable conditions.

**Growth of Fluorescent Silica on the Rods.** Stöber growth was used to coat silicon rods in two different experiments: the rods were coated either while dispersed as colloidal particles or before dispersing when they were still attached to the wafer.

In the first experiment, fluorescent silica growth on silicon particles according to the method of van Blaaderen[41] resulted in coated particles, with a layer of 50−100 nm fluorescently labeled silica. During growth of silica on the rods, silica particles formed as new nuclei since the rod concentration was low (~$2 \times 10^9$ particles). These secondary nucleated particles could easily be removed from the rods in repeated centrifugation with a table centrifuge (15 min, 750 rpm), by allowing the rods to sediment and refreshing the supernatant containing small particles. Figure 8 shows a HRTEM picture of a silica-coated silicon rod. The silica layer can be clearly distinguished from the silicon core. For example, the silicon core shows dark regions, likely stress induced during thermal oxidation. Also, the transition from the silicon core to the silica shell can be clearly identified by the change in atomic structure from ordered (crystalline silicon) to disordered (amorphous silica).

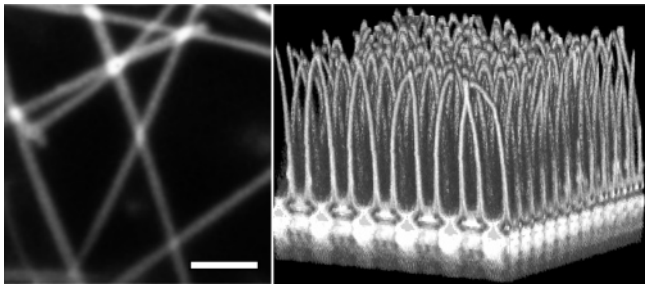

**Figure 9.** Fluorescence confocal microscopy images (488 nm excitation) of FITC-labeled silica rods in solution (left) and FITC-labeled silica rods on a wafer (right). (The scale bar represents 2.5 $\mu$m).

In the second experiment, a sample (1 $cm^2$) that was supercritically dried after the last etch step was then oxidized with the rods still attached to the wafer by placing it in the oven at 950 °C overnight. This resulted in free-standing silica rods with very few sintered connections. After that, the completely oxidized silica rods still on the wafer were coated with a fluorescent silica layer according to a method of Vossen and co-workers.[42] This method allows an accurate control of silica growth on the surface of small silicon structures by carrying out the growth in a dispersion of silica spheres. The amount of TEOS that was added was based on the combined surface area of the rods and the added 1030-nm spheres. Figure 9 shows a confocal microscope image of fluorescently labeled, silica-coated rods in a refractive index matching solution of 88% DMSO in water. The index-matched silica rods become translucent and the fluorescence intensity increases at the overlapping regions. This suggests that most, if not all, of the silicon has been thermally oxidized. These index-matched fluorescent rods will allow a 3D analysis of concentrated suspensions. An example of a reconstructed 3D image of fluorescent rods on the wafer is shown in Figure 9. A stack of scans in the focal plane parallel to the wafer (x−y) at different heights ($z$) was combined to obtain the 3D picture.

**Phase Behavior of Rods.** Suspensions of all-silicon rods in demineralized water were stable; no aggregated clusters of rods were found. This stability is very likely enhanced by monolayers of silica on the silicon surface ('native oxide'). After growth of a thin layer of fluorescent silica, the particles were charged and the interaction potential could be tuned by the salt concentration of the suspension; such suspensions were stable for at least several weeks. We looked at both thin and thick sediments of rods in water, which produced low and relatively high concentrations of rods, respectively. We also looked at sediments of diluted rod suspensions in highly deionized water (see Figure 10). The water was deionized by mixing it for at least 12 h with ion-exchange resin. It can be seen that, with increasing rod concentration in the suspension, the ordering in the sediment increases. At lower ion concentrations, particles will repel each other at larger distances since their charges are less screened. In this case, particles align at much lower concentrations and the ordered domains are larger than in water with higher ion concentration. These experiments show qualitatively the expected dependence of ordering effects on particle

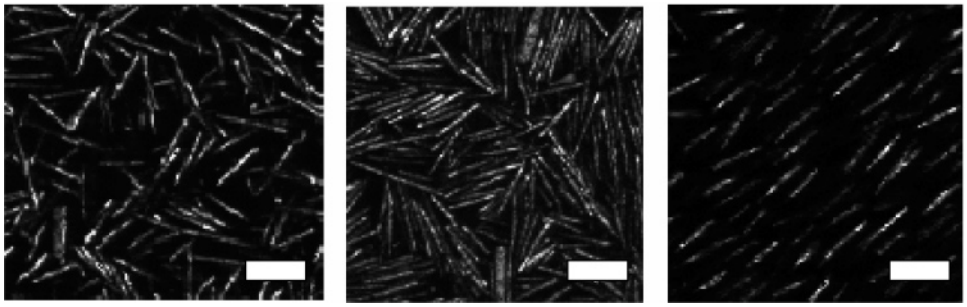

**Figure 10.** Confocal reflection images of sedimented silicon rods in water with low rod concentrations (left), high rod concentrations (middle), and low rod concentrations at low ionic strength after deionization (right). (The scale bar represents 5 $\mu$m).

concentration and charge. They show that we can control the particle interaction potential via the ion concentration.

In the future, full 3D analysis of ordered concentrated dispersions with FITC−silica-coated rods should be possible.

## IV. Conclusions and Outlook

We have shown that under the appropriate conditions it is possible to etch silicon rods from p-type silicon wafers and fine-tune their thickness by iterative oxidation and HF-etching steps. We succeeded in etching regular deep pores with alternating thickness in silicon wafers. The dimensions of these multisegmented structures can be well tuned and turned into single silicon rods that display liquid-crystalline phase behavior, with interesting properties for photonic applications. Coating of pure silica rods with a fluorescent layer opens a promising route to concentrated dispersions of these rods quantitatively in real space on a single-particle level.

**Acknowledgment.** John Kelly is thanked for useful discussions, Anton Kemmeren is thanked for his assistance in the etching experiments at Philips Research, and Maurits Weeda and Maxime Mellier are thanked for the explorative work on p-type silicon etching at Philips Research. Hans Meeldijk is thanked for the HRTEM measurements. This work was financially supported by the Foundation for the Fundamental Research of Matter (FOM), which is part of The Netherlands Organization for Scientific Research (NWO).

LA048817J